

The exclusive $B \rightarrow (K, K^*)\ell^+\ell^-$ decays in a CP softly broken two Higgs doublet model

Güray Erkol^{*} and Gürsevil Turan^{†‡}

Abstract

We study the differential branching ratio, forward-backward asymmetry, CP-violating asymmetry, CP-violating asymmetry in the forward-backward asymmetry and polarization asymmetries in the $B \rightarrow K\ell^+\ell^-$ and $B \rightarrow K^*\ell^+\ell^-$ decays in the context of a CP softly broken two Higgs doublet model. We analyze the dependencies of these observables on the model parameters by paying a special attention to the effects of neutral Higgs boson (NHB) exchanges and possible CP violating effects. We find that NHB effects are quite significant for both decays. A combined analysis of above-mentioned observables seems to be very promising as a testing ground for new physics beyond the SM, especially for the existence of the CP-violating phase in the theory.

1 Introduction

At the quark level, $B \rightarrow K^*\ell^+\ell^-$ and $B \rightarrow K\ell^+\ell^-$ decays ($\ell = e, \mu, \tau$) are induced by the $b \rightarrow s\ell^+\ell^-$ transition, which has received considerable attention [1]-[12], as a potential testing ground for the effective Hamiltonian describing the flavor changing neutral current processes in B decays. They are also expected to open a window to investigate the new physics prior to any possible experimental clue about it.

It is well known that the inclusive rare decays, although theoretically cleaner than the exclusive ones, are more difficult to measure. This fact stimulates the study of the exclusive decays, but the situation is contrary then: their experimental study is easy but the theoretical investigation is hard. For inclusive semileptonic B-meson decays, the physical observables can be calculated in heavy quark effective theory (HQET) [13]; however the description of the exclusive decays requires the additional knowledge of decay form factors, i.e., the matrix elements of the effective Hamiltonian between the initial B and final meson states. Finding these hadronic transition matrix elements is related to the nonperturbative sector of the QCD and should be calculated by means of a nonperturbative approach. The form factors for B decays into K and K^* have been calculated in the framework of different methods, such as chiral theory [14], three point QCD sum rules method [15], relativistic quark model [16], effective heavy quark theory [17], and light cone sum rules [18], [19].

^{*}E-mail address: gurerk@newton.physics.metu.edu.tr

[†]E-mail address: gsevgur@metu.edu.tr

[‡]Common address: Middle East Technical University Physics Dept. Inonu Bul. 06531 Ankara-TURKEY

From the experimental side, there exist upper limits on the branching ratios of $B^0 \rightarrow K^{0*} \mu^+ \mu^-$ and $B^+ \rightarrow K^+ \mu^+ \mu^-$, given by CDF collaboration [20]

$$\begin{aligned} BR(B^0 \rightarrow K^{0*} \mu^+ \mu^-) &< 4.0 \times 10^{-6} \\ BR(B^+ \rightarrow K^+ \mu^+ \mu^-) &< 5.2 \times 10^{-6}. \end{aligned}$$

With these measured upper limits and also the recent measurement of the branching ratio of $B \rightarrow K \ell^+ \ell^-$ with $\ell = e, \mu$,

$$BR(B \rightarrow K \ell^+ \ell^-) = (0.75_{-0.21}^{+0.25} \pm 0.09) \times 10^{-6},$$

at KEK [21], the processes $B \rightarrow (K, K^*) \ell^+ \ell^-$ have received great interest so that their theoretical calculation has been the subject of many investigations in the SM and beyond, such as the SM with fourth generation, multi-Higgs doublet models, minimal supersymmetric extension of the SM (MSSM) and in a model independent method [22]-[37].

In this paper we will investigate the exclusive $B \rightarrow (K, K^*) \ell^+ \ell^-$ decays in a CP softly broken two Higgs doublet model, which is called model IV in the literature [39].

CP violating asymmetry A_{CP} is an important observable that may provide valuable information about the models used. In the SM the source of CP violation is the complex Cabibbo-Kobayashi-Maskawa (CKM) matrix elements and due to unitarity of this matrix together with the smallness of the term $V_{ub}V_{us}^*$, A_{CP} for $B \rightarrow (K, K^*) \ell^+ \ell^-$ decays almost vanishes in the SM. However, like many extensions of the SM, model IV predicts a new source of CP violation so that we have an opportunity to investigate the physics beyond the SM by analysing the CP violating effects.

In model IV, up-type quarks get masses from Yukawa couplings to the one Higgs doublet H_2 , and down-type quarks and leptons get masses from another Higgs doublet H_1 . In such a 2HDM, all the parameters in the Higgs potential are real so that it is CP-conserving, but one allows the real and imaginary parts of $\phi_1^+ \phi_2$ to have different self-couplings so that the phase ξ , which comes from the expectation value of Higgs field, can not be rotated away, which breaks the CP symmetry (for details, see ref [39]). In model IV, interaction vertices of the Higgs bosons and the down-type quarks and leptons depend on the CP violating phase ξ and the ratio $\tan \beta = v_2/v_1$, where v_1 and v_2 are the vacuum expectation values of the first and the second Higgs doublet respectively, and they are free parameters in the model. The constraints on $\tan \beta$ are usually obtained from $B - \bar{B}$, $K - \bar{K}$ mixing, $b \rightarrow s \gamma$ decay width, semileptonic decay $b \rightarrow c \tau \bar{\nu}$ and is given by [40]

$$0.7 \leq \tan \beta \leq 0.52 \left(\frac{m_{H^\pm}}{1 \text{ GeV}} \right), \quad (1)$$

and the lower bound $m_{H^\pm} \geq 200 \text{ GeV}$ has also been given in [40].

In addition to the CP asymmetry A_{CP} , differential or total branching ratios and the forward-backward asymmetries, polarization asymmetries are also thought to play an important role in further investigations of the structure of the SM and for establishing new physics beyond it. It has been pointed out in refs.[10] and [28] that the longitudinal polarization P_L of the final lepton may be accessible in the $B \rightarrow (K, K^*) \tau^+ \tau^-$ mode in the near future. It has been shown [12] that together with P_L , the other two orthogonal components of polarization, P_T and P_N , are crucial for the $\tau^+ \tau^-$ mode since these three components contain the independent, but complementary information because they involve different combinations of Wilson coefficients in addition to the fact that they are proportional to m_ℓ/m_b . Lepton polarizations in $B \rightarrow K(K^*) \ell^+ \ell^-$ decays are analyzed in the model II version of the 2HDM and in a general model independent way in refs.[30] ([35]) and [41] ([42]), respectively. Ref.[43] gives an analysis of the lepton polarization asymmetries in the processes $B \rightarrow (K, K^*) \ell^+ \ell^-$ in a supersymmetric context.

As pointed out before, (see f.eg.[44]-[48]), in models with two Higgs doublets, like MSSM, 2HDM, etc., neutral Higgs boson (NHB) effects could contribute largely to the semileptonic rare B meson decays, especially for heavy lepton modes and for large $\tan\beta$. However, in the literature there was a disagreement about the results of NHB exchange diagrams contributing to $b \rightarrow s \ell^+ \ell^-$ transition in the context of the 2HDM [46, 47]. This situation seems to be resolved now [47, 49], and in view of new forms of the Wilson coefficients C_{Q_1} and $C_{\bar{Q}_1}$ due to NHB effects, it is quite worthwhile to return to the exclusive processes $B \rightarrow (K, K^*) \tau^+ \tau^-$ in order to investigate the NHB effects together with the CP violating effects in model IV.

The paper is organized as follows: In Sec. 2, after we give the effective Hamiltonian and the definitions of the form factors, we introduce basic formulas of observables. Sec. 3 is devoted to the numerical analysis and discussion of our results.

2 Effective Hamiltonian and form factors

At the quark level, the effective Hamiltonian describing the rare semileptonic $b \rightarrow s \ell^+ \ell^-$ transition can be obtained by integrating out the top quark, Higgs bosons and W^\pm , Z bosons:

$$\mathcal{H}_{eff} = \frac{4G_F}{\sqrt{2}} V_{tb} V_{ts}^* \left(\sum_{i=1}^{10} C_i(\mu) O_i(\mu) + \sum_{i=1}^{10} C_{Q_i}(\mu) Q_i(\mu) \right), \quad (2)$$

where O_i are current-current ($i = 1, 2$), penguin ($i = 1, \dots, 6$), magnetic penguin ($i = 7, 8$) and semileptonic ($i = 9, 10$) operators and $C_i(\mu)$ are the corresponding Wilson coefficients renormalized at the scale μ [50, 51]. The additional operators Q_i , ($i = 1, \dots, 10$) and their Wilson coefficients are due to the NHB exchange diagrams, which can be found in [45, 47, 49].

Neglecting the mass of the s quark, the above Hamiltonian leads to the following matrix element:

$$\begin{aligned} \mathcal{M} = & \frac{G_F \alpha}{2\sqrt{2}\pi} V_{tb} V_{ts}^* \left\{ C_9^{eff} \bar{s} \gamma_\mu (1 - \gamma_5) b \bar{\ell} \gamma^\mu \ell + C_{10} \bar{s} \gamma_\mu (1 - \gamma_5) b \bar{\ell} \gamma^\mu \gamma_5 \ell \right. \\ & \left. - 2C_7^{eff} \frac{m_b}{q^2} \bar{s} i \sigma_{\mu\nu} q^\nu (1 + \gamma_5) b \bar{\ell} \gamma^\mu \ell \right\}, \end{aligned} \quad (3)$$

where q is the momentum transfer. Here, Wilson coefficient $C_9^{eff}(\mu)$ contains a perturbative part and a part coming from long-distance effects due to conversion of the real $\bar{c}c$ into lepton pair $\ell^+ \ell^-$:

$$C_9^{eff}(\mu) = C_9^{pert}(\mu) + Y_{reson}(s), \quad (4)$$

where

$$\begin{aligned} C_9^{pert}(\mu) = & C_9^{2HDM}(\mu) \\ & + h(z, s) [3C_1(\mu) + C_2(\mu) + 3C_3(\mu) + C_4(\mu) + 3C_5(\mu) + C_6(\mu)] \\ & - \frac{1}{2} h(1, s) (4C_3(\mu) + 4C_4(\mu) + 3C_5(\mu) + C_6(\mu)) \\ & - \frac{1}{2} h(0, s) [C_3(\mu) + 3C_4(\mu)] \\ & + \frac{2}{9} (3C_3(\mu) + C_4(\mu) + 3C_5(\mu) + C_6(\mu)), \end{aligned} \quad (5)$$

and $z = m_c/m_b$. The functions $h(z, s)$ arises from the one loop contributions of the four quark operators O_1, \dots, O_6 and their explicit forms can be found in [51]. It is possible to parametrize the resonance $\bar{c}c$ contribution $Y_{reson}(s)$ in Eq.(4) using a Breit-Wigner shape with normalizations fixed by data which is given by [52]

$$Y_{reson}(s) = -\frac{3}{\alpha_{em}^2} \kappa \sum_{V_i=\psi_i} \frac{\pi \Gamma(V_i \rightarrow \ell^+ \ell^-) m_{V_i}}{s m_B^2 - m_{V_i}^2 + i m_{V_i} \Gamma_{V_i}} \times [(3C_1(\mu) + C_2(\mu) + 3C_3(\mu) + C_4(\mu) + 3C_5(\mu) + C_6(\mu))]. \quad (6)$$

The phenomenological parameter κ in Eq. (6) is taken as 2.3 so as to reproduce the correct value of the branching ratio $BR(B \rightarrow J/\psi X \rightarrow X \ell \bar{\ell}) = BR(B \rightarrow J/\psi X) BR(J/\psi \rightarrow X \ell \bar{\ell})$.

Next we proceed to calculate the differential branching ratio dBR/ds , forward-backward asymmetry A_{FB} , CP violating asymmetry A_{CP} , CP asymmetry in the forward-backward asymmetry $A_{CP}(A_{FB})$ and finally the lepton polarization asymmetries of the $B \rightarrow K \ell^+ \ell^-$ and $B \rightarrow K^* \ell^+ \ell^-$ decays. In order to find these physically measurable quantities at hadronic level, the necessary matrix elements are $\langle M(p_M) | \bar{s} \gamma_\mu (1 - \gamma_5) b | B(p_B) \rangle$, $\langle M(p_M) | \bar{s} i \sigma_{\mu\nu} q_\nu (1 + \gamma_5) b | B(p_B) \rangle$ and $\langle M(p_M) | \bar{s} (1 + \gamma_5) b | B(p_B) \rangle$ for $M = K, K^*$, which can be parametrized in terms of form factors. Using the parametrization of the form factors as in [30] and [32], we find the amplitudes governing the $B \rightarrow K \ell^+ \ell^-$ and the $B \rightarrow K^* \ell^+ \ell^-$ decays as follows:

$$\mathcal{M}^{B \rightarrow K} = \frac{G_F \alpha}{2\sqrt{2}\pi} V_{tb} V_{ts}^* \left\{ [2A_1 p_K^\mu + B_1 q^\mu] \bar{\ell} \gamma_\mu \ell + [2G_1 p^\mu + D_1 q^\mu] \bar{\ell} \gamma_\mu \gamma_5 \ell + E_1 \bar{\ell} \ell + F_1 \bar{\ell} \gamma_5 \ell \right\}, \quad (7)$$

and

$$\begin{aligned} \mathcal{M}^{B \rightarrow K^*} = & \frac{G_F \alpha}{2\sqrt{2}\pi} V_{tb} V_{ts}^* \left\{ \bar{\ell} \gamma_\mu \ell [2A \epsilon_{\mu\nu\lambda\sigma} \varepsilon^{*\nu} p_{K^*}^\lambda p_B^\sigma + iB \varepsilon_\mu^* - iC(p_B + p_{K^*})_\mu (\varepsilon^* q) - iD(\varepsilon^* q) q_\mu] \right. \\ & + \bar{\ell} \gamma_\mu \gamma_5 \ell [2E \epsilon_{\mu\nu\lambda\sigma} \varepsilon^{*\nu} p_{K^*}^\lambda p_B^\sigma + iF \varepsilon_\mu^* - iG(\varepsilon^* q)(p_B + p_{K^*}) - iH(\varepsilon^* q) q_\mu] + i\bar{\ell} \ell Q(\varepsilon^* q) \\ & \left. + i\bar{\ell} \gamma_5 \ell N(\varepsilon^* q) \right\} \end{aligned} \quad (8)$$

where

$$\begin{aligned} A_1 &= C_9^{eff} f^+ - 2m_B C_7^{eff} \frac{f_T}{m_B + m_K}, \\ B_1 &= C_9^{eff} (f^+ + f^-) + 2C_7^{eff} \frac{m_B}{q^2} f_T \frac{(m_B^2 - m^2 - q^2)}{m_B + m_K}, \\ G_1 &= C_{10} f^+, \\ D_1 &= C_{10} (f^+ + f^-), \\ E_1 &= C_{Q1} \frac{1}{m_b} [(m_B^2 - m_K^2) f^+ + f^- q^2], \\ F_1 &= C_{Q2} \frac{1}{m_b} [(m_B^2 - m_K^2) f^+ + f^- q^2], \\ A &= C_9^{eff} \frac{V}{m_B + m_{K^*}} + 4 \frac{m_b}{q^2} C_7^{eff} T_1, \\ B &= (m_B + m_{K^*}) \left(C_9^{eff} A_1 + \frac{4m_b}{q^2} (m_B - m_{K^*}) C_7^{eff} T_2 \right), \end{aligned}$$

$$\begin{aligned}
C &= C_9^{eff} \frac{A_2}{m_B + m_{K^*}} + 4 \frac{m_b}{q^2} C_7^{eff} \left(T_2 + \frac{q^2}{m_B^2 - m_{K^*}^2} T_3 \right), \\
D &= 2C_9^{eff} \frac{m_{K^*}}{q^2} (A_3 - A_0) - 4C_7^{eff} \frac{m_b}{q^2} T_3, \\
E &= C_{10} \frac{V}{m_B + m_{K^*}}, \\
F &= C_{10} (m_B + m_{K^*}) A_1, \\
G &= C_{10} \frac{A_2}{m_B + m_{K^*}}, \\
H &= 2C_{10} \frac{m_{K^*}}{q^2} (A_3 - A_0), \\
Q &= 2C_{Q1} \frac{m_{K^*}}{m_b} A_0, \\
N &= 2C_{Q2} \frac{m_{K^*}}{m_b} A_0.
\end{aligned} \tag{9}$$

Here f^+ , f^- and f_T and A_0 , A_1 , A_2 , A_3 , V , T_1 , T_2 and T_3 are the relevant form factors in $B \rightarrow K$ and $B \rightarrow K^*$ transitions, respectively. For $B \rightarrow K$, we use the results calculated in the light cone QCD sum rules framework, which can be written in the following pole forms [30]

$$\begin{aligned}
f^+(q^2) &= \frac{0.29}{\left(1 - \frac{q^2}{23.7}\right)}, \\
f^-(q^2) &= -\frac{0.21}{\left(1 - \frac{q^2}{24.3}\right)}, \\
f_T(q^2) &= -\frac{0.31}{\left(1 - \frac{q^2}{23}\right)},
\end{aligned} \tag{10}$$

As for the $B \rightarrow K^*$ transition, we use the result of [19], where q^2 dependence of the form factors can be represented in terms of three parameters as given by

$$F(q^2) = \frac{F(0)}{1 - a_F \frac{q^2}{m_B^2} + b_F \left(\frac{q^2}{m_B^2}\right)^2},$$

where the values of parameters $F(0)$, a_F and b_F for the $B \rightarrow K^*$ decay are listed in Table 1. The form factors A_0 and A_3 in Eq. (9) can be found from the following parametrization,

$$\begin{aligned}
A_0 &= A_3 - \frac{T_3 q^2}{m_{K^*} m_b}, \\
A_3 &= \frac{m_B + m_{K^*}}{2m_{K^*}} A_1 - \frac{m_B - m_{K^*}}{2m_{K^*}} A_2.
\end{aligned} \tag{11}$$

Using Eqs. (7) and (8) and performing summation over final lepton polarization, we get for the double differential decay rates:

$$\frac{d^2 \Gamma^{B \rightarrow K}}{ds dz} = \frac{G_F^2 \alpha^2}{2^{11} \pi^5} |V_{tb} V_{ts}^*|^2 m_B^3 \sqrt{\lambda} v \left\{ m_B^2 \lambda (1 - z^2 v^2) |A_1|^2 + s(v^2 |E_1|^2 + |F_1|^2) \right\}$$

	$F(0)$	a_F	b_F
$A_1^{B \rightarrow K^*}$	0.34 ± 0.05	0.60	-0.023
$A_2^{B \rightarrow K^*}$	0.28 ± 0.04	1.18	0.281
$V^{B \rightarrow K^*}$	0.46 ± 0.07	1.55	0.575
$T_1^{B \rightarrow K^*}$	0.19 ± 0.03	1.59	0.615
$T_2^{B \rightarrow K^*}$	0.19 ± 0.03	0.49	-0.241
$T_3^{B \rightarrow K^*}$	0.13 ± 0.02	1.20	0.098

Table 1: $B \rightarrow K^*$ transition form factors in light cone QCD sum rules .

$$\begin{aligned}
& + (m_B^2 \lambda (1 - z^2 v^2) + 16 r m_\ell^2) |G_1|^2 + 4 s m_\ell^2 |D_1|^2 \\
& + 4 m_\ell^2 (1 - r - s) \text{Re}[G_1 D_1^*] + 2 v m_\ell \sqrt{\lambda} z \text{Re}[A_1 E_1^*] \\
& + 2 m_\ell ((1 - r - s) \text{Re}[G_1 F_1^*] + s \text{Re}[D_1 F_1^*]) \Big\} , \tag{12}
\end{aligned}$$

and

$$\begin{aligned}
\frac{d^2 \Gamma^{B \rightarrow K^*}}{ds dz} &= \frac{\alpha^2 G_F^2}{2^{15} m_B \pi^5} |V_{tb} V_{ts}^*|^2 \sqrt{\lambda_*} v \Big\{ 4 s \lambda_* (2 + v^2 (z^2 - 1)) |A|^2 \\
& + 4 v^2 s m_B^4 \lambda_* (1 + z^2) |E|^2 + 16 m_B^2 s v z \sqrt{\lambda_*} (\text{Re}[B E^*] + \text{Re}[A F^*]) \\
& + \frac{1}{r} \Big[\lambda_* (1 - z^2 v^2) + 2 r_* s (5 - 2 v^2) \Big] |B|^2 + m_B^4 \lambda_*^2 (1 - z^2 v^2) |C|^2 \\
& + [\lambda_* (1 - z^2 v^2) - 2 r_* s (1 - 4 v^2)] |F|^2 + m_B^4 \lambda_* [(-1 + r_*)^2 (1 - v^2) z^2 \\
& + (-1 + z^2) (s t^2 - 8(1 + r_*) t^2 - \lambda_*)] |G|^2 + 2 m_B^2 \lambda_* W_* (1 - z^2 v^2) \text{Re}[B C^*] \\
& - 2 m_B^2 \lambda_* [W_* (1 - z^2 v^2) - 4 t^2] \text{Re}[F G^*] + m_B^2 \lambda_* (4 s m_\ell (m_\ell |H|^2 + \text{Re}[H N^*]) \\
& + s(|N|^2 + v^2 |Q|^2) - 4 t (\text{Re}[F(2 t H^* + N^*/m_B)] \\
& + 4(1 - r_*) m_\ell \text{Re}[G(2 m_\ell H^* + N^*)]) \\
& + 4 t m_B v z^2 \text{Re}[(W_* B + m_B^2 (W_*^2 - 4 r_* s) C) Q^*] \Big\} . \tag{13}
\end{aligned}$$

Here $s = q^2/m_B^2$, $r_{(*)} = m_{K(K^*)}^2/m_B^2$, $v = \sqrt{1 - \frac{4t^2}{s}}$, $t = m_l/m_B$, $\lambda_{(*)} = r_{(*)}^2 + (s - 1)^2 - 2r_{(*)}(s + 1)$, $W_{(*)} = -1 + r_{(*)} + s$ and $z = \cos \theta$, where θ is the angle between the three-momentum of the ℓ^- lepton and that of the B-meson in the center of mass frame of the dileptons $\ell^+ \ell^-$.

Having established the double differential decay rates, let us now consider the forward-backward asymmetry A_{FB} of the lepton pair, which is defined as

$$A_{FB}(s) = \frac{\int_0^1 dz \frac{d^2 \Gamma}{ds dz} - \int_{-1}^0 dz \frac{d^2 \Gamma}{ds dz}}{\int_0^1 dz \frac{d^2 \Gamma}{ds dz} + \int_{-1}^0 dz \frac{d^2 \Gamma}{ds dz}} . \tag{14}$$

The A_{FB} 's for the $B \rightarrow K \ell^+ \ell^-$ and $B \rightarrow K^* \ell^+ \ell^-$ decays are calculated to be

$$A_{FB}^{B \rightarrow K} = - \int ds (tv^2 \lambda \text{Re}(A_1 E_1^*)) \Big/ \int ds v \sqrt{\lambda} \Delta, \quad (15)$$

$$\begin{aligned} A_{FB}^{B \rightarrow K^*} &= \int ds 2m_B^3 \lambda_* v^2 \left(4m_B s (\text{Re}[B E^*] + \text{Re}[A F^*]) \right. \\ &\quad \left. + \frac{t}{r_*} [W_* \text{Re}[B Q^*] + m_B^2 \lambda_* \text{Re}[C Q^*]] \right) \Big/ \int ds \sqrt{\lambda_*} v \Delta_*. \end{aligned} \quad (16)$$

We note that in the SM, A_{FB} in $B \rightarrow K \ell^+ \ell^-$ decay is zero because of the fact that hadronic current for $B \rightarrow K$ transition does not have any axial counterpart. As seen from Eq.(15), it is also zero in model IV unless we do not take into effect the NHB exchanges. Therefore, $B \rightarrow K \ell^+ \ell^-$ decay may be a good candidate for testing the existence and the importance of NHB effects.

In this work, we also analyse the CP violating asymmetry A_{CP} , which is defined as

$$A_{CP} = \frac{d\Gamma/ds(B \rightarrow M \ell^+ \ell^-) - d\Gamma/ds(\bar{B} \rightarrow \bar{M} \ell^+ \ell^-)}{d\Gamma/ds(B \rightarrow M \ell^+ \ell^-) + d\Gamma/ds(\bar{B} \rightarrow \bar{M} \ell^+ \ell^-)}. \quad (17)$$

where $M = K, K^*$ and $d\Gamma/ds$ are the corresponding differential decay rates, which are obtained by integrating the expressions in Eqs. (12) and (13) over the angle variable

$$\frac{d\Gamma^{B \rightarrow K}}{ds} = \frac{G_F^2 \alpha^2}{2^{10} \pi^5} |V_{tb} V_{ts}^*|^2 m_B^3 \sqrt{\lambda} v \Delta, \quad (18)$$

where

$$\begin{aligned} \Delta &= \frac{1}{3} m_B^2 \lambda (3 - v^2) (|A_1|^2 + |G_1|^2) + \frac{4m_\ell^2}{3s} (12r s + \lambda) |G_1|^2 \\ &\quad + 4 m_\ell^2 s |D_1|^2 + s(v^2 |E_1|^2 + |F_1|^2) + 4 m_\ell^2 (1 - r - s) \text{Re}[G_1 D_1^*] \\ &\quad + 2 m_\ell ((1 - r - s) \text{Re}[G_1 F_1^*] + s \text{Re}[D_1 F_1^*]), \end{aligned} \quad (19)$$

and

$$\frac{d\Gamma^{B \rightarrow K^*}}{ds} = \frac{\alpha^2 G_F^2 m_B}{2^{12} \pi^5} |V_{tb} V_{ts}^*|^2 \sqrt{\lambda_*} v \Delta_*. \quad (20)$$

where

$$\begin{aligned} \Delta_* &= \frac{8}{3} \lambda_* m_B^6 s ((3 - v^2) |A|^2 + 2v^2 |E|^2) - \frac{4}{r} \lambda_* m_B^2 m_\ell \text{Re}[(F - m_B^2 (1 - r_*) G - m_B^2 s H) N^*] \\ &\quad + \frac{1}{r_*} \lambda_* m_B^4 \left[s v^2 |Q|^2 + \frac{1}{3} \lambda_* m_B^2 (3 - v^2) |C|^2 + s |N|^2 + m_B^2 s^2 (1 - v^2) |H|^2 \right. \\ &\quad + \frac{2}{3} [(3 - v^2) W_* - 3s(1 - v^2)] \text{Re}[F G^*] - 2s(1 - v^2) \text{Re}[F H^*] \\ &\quad \left. + 2m_B^2 s (1 - r_*) (1 - v^2) \text{Re}[G H^*] + \frac{2}{3} (3 - v^2) W_* \text{Re}[B C^*] \right] \\ &\quad + \frac{1}{3r_*} m_B^2 \left[(\lambda_* + 12r_* s) (3 - v^2) |B|^2 + \lambda_* m_B^4 [\lambda_* (3 - v^2) \right. \\ &\quad \left. - 3s(s - 2r_* - 2)(1 - v^2)] |G|^2 + (\lambda_* (3 - v^2) + 24r_* s v^2) |F|^2 \right]. \end{aligned} \quad (21)$$

We would also like to present the CP asymmetry in the forward-backward asymmetry $A_{CP}(A_{FB})$, which is another observable that can give information about the physics beyond the SM. It is defined as

$$A_{CP}(A_{FB}) = \frac{A_{FB} - \bar{A}_{FB}}{A_{FB} + \bar{A}_{FB}}. \quad (22)$$

where \bar{A}_{FB} is the CP conjugate of A_{FB} .

Finally, we would like to discuss the lepton polarization effects for the $B \rightarrow K \ell^+ \ell^-$ and $B \rightarrow K^* \ell^+ \ell^-$ decays. The polarization asymmetries of the final lepton is defined as

$$P_n(s) = \frac{(d\Gamma(S_n)/ds) - (d\Gamma(-S_n)/ds)}{(d\Gamma(S_n)/ds) + (d\Gamma(-S_n)/ds)} \quad (23)$$

for $n = L, N, T$. Here, P_L, P_T and P_N are the longitudinal, transversal and normal polarizations, respectively. The unit vectors S_n are defined as follows:

$$\begin{aligned} S_L &= (0, \vec{e}_L) = \left(0, \frac{\vec{p}_+}{|\vec{p}_+|}\right) \\ S_N &= (0, \vec{e}_N) = \left(0, \frac{\vec{p} \times \vec{p}_+}{|\vec{p} \times \vec{p}_+|}\right) \\ S_T &= (0, \vec{e}_T) = \left(0, \vec{e}_N \times \vec{e}_L\right), \end{aligned} \quad (24)$$

where $\vec{p} = \vec{p}_K, \vec{p}_{K^*}$ and \vec{p}_+ are the three-momenta of K, K^* and ℓ^+ , respectively. The longitudinal unit vector S_L is boosted to the CM frame of $\ell^+ \ell^-$ by Lorentz transformation:

$$S_{L,CM} = \left(\frac{|\vec{p}_+|}{m_\ell}, \frac{E_\ell \vec{p}_+}{m_\ell |\vec{p}_+|}\right). \quad (25)$$

It follows from the definition of unit vectors S_n that P_T lies in the decay plane while P_N is perpendicular to it, and they are not changed by the boost.

After some algebra, we obtain the following expressions for the polarization components of the ℓ^+ lepton in $B \rightarrow K \ell^+ \ell^-$ and $B \rightarrow K^* \ell^+ \ell^-$ decays:

$$\begin{aligned} P_L^{B \rightarrow K} &= \frac{4m_B^3 v}{3\Delta} \left(-2m_B \lambda \text{Re}[A_1 G_1^*] - 6t(1-r-s) \text{Re}[G_1 E_1^*] - 6st \text{Re}[D_1 E_1^*] \right. \\ &\quad \left. + 3s \text{Re}[E_1 F_1^*] \right), \\ P_T^{B \rightarrow K} &= \frac{m_B^3 \pi \sqrt{\lambda}}{\sqrt{s} \Delta} \left(-2m_B(1-r-s)t \text{Re}[A_1 G_1^*] - 2m_B st \text{Re}[A_1 D_1^*] \right. \\ &\quad \left. + (s-4t^2) \text{Re}[G_1 E_1^*] + s \text{Re}[A_1 F_1^*] \right), \\ P_N^{B \rightarrow K} &= \frac{m_B^3 \pi v \sqrt{s} \lambda}{\Delta} \left(2m_B t \text{Im}[G_1 D_1^*] - \text{Im}[A_1 E_1^*] - \text{Im}[G_1 F_1^*] \right), \end{aligned} \quad (26)$$

and

$$P_L^{B \rightarrow K^*} = \frac{4m_B^2 v}{r_* \Delta_*} \left(\lambda_* m_B t \text{Re}[(-F + m_B^2(1-r_*)G + m_B^2 s H) Q^*] \right)$$

$$\begin{aligned}
& + \frac{8}{3} \lambda m_B^4 r_* s \text{Re}[A E^*] - \frac{1}{3} \text{Re}[B (\lambda m_B^2 (1 - r_* - s) G^* - (\lambda + 12 r_* s) F^*) \\
& + C (\lambda m_B^2 (1 - r_* - s) F^* - \lambda^2 m_B^4 G^*)] + \frac{1}{2} \lambda_* m_B^2 s \text{Re}[Q N^*] \Big), \\
P_T^{B \rightarrow K^*} &= \frac{\pi m_B^2 \sqrt{\lambda_*}}{\Delta_* r \sqrt{s}} \Big(8 m_B^2 r_* s t \text{Re}[A B^*] - m_B^2 t (1 - r_*) [(1 - r_* - s) \text{Re}[B G^*] \\
& - \lambda_* m_B^2 \text{Re}[C G^*]] - \lambda_* m_B^2 t \text{Re}[F C^*] - \frac{1}{2} m_B s \text{Re}[(B(1 - r_* - s) - \lambda_* m_B^2 C) N^*] \\
& + \lambda_* m_B^4 s t \text{Re}[C H^*] + \frac{1}{2} s m_B v^2 \text{Re}[(F(1 - r_* - s) - \lambda_* m_B^2 G) Q^*] \\
& - t(1 - r_* - s) \text{Re}[(m_B^2 s H - F) B^*] \Big), \\
P_N^{B \rightarrow K^*} &= \frac{\pi m_B^3 v \sqrt{s \lambda}}{\Delta_* r_*} \Big(4 m_B t r_* \text{Im}[B E^* + A F^*] + \frac{1}{2} \lambda_* m_B^2 \text{Im}[-2 m_B t H^* G \\
& - G N^* + C Q^*] - (1 + 3 r_* - s) m_B t \text{Im}[G F^*] \\
& - (1 - r_* - s) \text{Im}[m_B t H F^* - \frac{1}{2} N F^* + \frac{1}{2} Q B^*] \Big).
\end{aligned}$$

3 Numerical results and discussion

In this section we present the numerical analysis of the exclusive decays $B \rightarrow K \ell^+ \ell^-$ and $B \rightarrow K^* \ell^+ \ell^-$ in model IV. We will give the results for only $\ell = \tau$ channel, which demonstrates the NHB effects more manifestly. The input parameters we used in this analysis are as follows:

$$\begin{aligned}
m_K &= 0.493 \text{ GeV}, & m_B &= 5.28 \text{ GeV}, & m_b &= 4.8 \text{ GeV}, & m_c &= 1.4 \text{ GeV}, & m_\tau &= 1.77 \text{ GeV}, \\
m_{K^*} &= 0.893 \text{ GeV}, & m_{H^\pm} &= 250 \text{ GeV}, & m_{H^0} &= 125 \text{ GeV}, & m_{h^0} &= 100 \text{ GeV} \\
|V_{tb} V_{ts}^*| &= 0.04, & \alpha^{-1} &= 129, & G_F &= 1.17 \times 10^{-5} \text{ GeV}^{-2}, & \tau_B &= 1.64 \times 10^{-12} \text{ s}.
\end{aligned} \quad (27)$$

The masses of the charged and neutral Higgs bosons, m_{H^\pm} , m_{H^0} , m_{A^0} and m_{h^0} , and the ratio of the vacuum expectation values of the two Higgs doublets, $\tan \beta$, remain as free parameters of the model. The restrictions on m_{H^\pm} , and $\tan \beta$ have been already discussed in section 1. For the masses of the neutral Higgs bosons, the lower limits are given as $m_{H^0} \geq 115 \text{ GeV}$, $m_{h^0} \geq 89.9 \text{ GeV}$ and $m_{A^0} \geq 90.1 \text{ GeV}$ in [53].

Before we present our results, a small note about the calculations of the long-distance effects is in order. There are five possible resonances in the $c\bar{c}$ system that can contribute to the decays under consideration and to calculate them, we need to divide the integration region for s into two parts so that we have

$$4m_\ell^2/m_B^2 \leq s \leq (m_{\psi_2} - 0.02)^2/m_B^2, \quad (m_{\psi_2} + 0.02)^2/m_B^2 \leq s \leq (m_B - m_M)^2/m_B^2, \quad (28)$$

where $m_{\psi_2} = 3.686 \text{ GeV}$ is the mass of the second resonance, and $M = K, K^*$.

In the following, we give results of our calculations about the dependencies of the differential branching ratio dBR/ds , forward-backward asymmetry $A_{FB}(s)$, CP violating asymmetry $A_{CP}(s)$, CP asymmetry in the forward-backward asymmetry $A_{CP}(A_{FB})(s)$ and finally the components of the lepton polarization asymmetries, $P_L(s)$, $P_T(s)$ and $P_N(s)$, of the $B \rightarrow K \tau^+ \tau^-$ and $B \rightarrow K^* \tau^+ \tau^-$ decays on the invariant dilepton mass s . In order to investigate the dependencies of the above physical quantities on the model parameters, namely CP violating phase

ξ and $\tan\beta$, we eliminate the other parameter s by performing the s integrations over the allowed kinematical region (Eq.(28)) so as to obtain their averaged values, $\langle A_{FB} \rangle$, $\langle A_{CP} \rangle$, $\langle A_{CP}(A_{FB}) \rangle$, $\langle P_L \rangle$, $\langle P_T \rangle$ and $\langle P_N \rangle$.

Numerical results are shown in Figs. (1)-(26) and we have the following line conventions: dot lines, dashed-dot lines and solid lines represent the model IV contributions with $\tan\beta = 10, 30, 50$, respectively and the dashed lines are for the SM predictions. The cases of switching off NHB contributions i.e., setting $C_{Q_i} = 0$, almost coincide with the cases of 2HDM contributions with $\tan\beta = 10$, therefore we did not plot them separately.

In Fig.(1), we give the dependence of the dBR/ds on s for $B \rightarrow K \tau^+ \tau^-$. From this figure NHB effects are very obviously seen, especially in the high- s region.

In Fig. (2) and Fig. (3), $A_{FB}(s)$ and $\langle A_{FB} \rangle$ of $B \rightarrow K \tau^+ \tau^-$ as a function of s and CP violating phase ξ are presented. Since A_{FB} arises in the 2HDM only when NHB effects are taken into account, it provides a good probe to test these effects. We see that A_{FB} is quite sensitive to $\tan\beta$ and it is negative for all values of ξ and s except in the ψ region. $\langle A_{FB} \rangle$ in $B \rightarrow K \tau^+ \tau^-$ is between $(-0.04, -0.01)$, which is non zero but hard to observe.

Fig. (4) and Fig. (5) show the dependence of $A_{CP}(s)$ on s and $\langle A_{CP} \rangle$ on ξ for $B \rightarrow K \tau^+ \tau^-$ decay. We see that $A_{CP}(s)$ is quite sensitive to $\tan\beta$ and its sign does not change in the allowed values of s except in the resonance mass region of ψ when $\tan\beta = 50$. It follows from Fig. (5) that $\langle A_{CP} \rangle$ is also sensitive to ξ , and it varies in the range $(-0.8, 0.8) \times 10^{-2}$, which may provide an indication for the existence of new physics since A_{CP} is zero in the SM.

$A_{CP}(A_{FB})(s)$ and $\langle A_{CP}(A_{FB}) \rangle$ of $B \rightarrow K \ell^+ \ell^-$ as a function of s and CP violating phase ξ are presented in Fig. (6) and Fig. (7), respectively. We note that in both of these figures, predictions for the different values of $\tan\beta$ completely coincide which indicates that $A_{CP}(A_{FB})$ is not sensitive to this parameter in $B \rightarrow K \tau^+ \tau^-$ decay. As seen from Fig. (7), $\langle A_{CP}(A_{FB}) \rangle$ strongly depends on CP violating phase ξ and it can reach about 6% for some values of ξ .

In Figs. (8)-(10), we present the s dependence of the longitudinal P_L , transverse P_T and normal P_N polarizations of the final lepton for $B \rightarrow K \tau^+ \tau^-$ decay. We see that except the ψ region, P_N is negative for all values of s , but P_L and P_T change sign with the different choices of the values of $\tan\beta$. The effects of NHB exchanges are also very obvious. In Figs. (11)-(13), dependence of the averaged values of the longitudinal $\langle P_L \rangle$, transverse $\langle P_T \rangle$ and normal $\langle P_N \rangle$ polarizations of the final lepton for $B \rightarrow K \ell^+ \ell^-$ decay on ξ are shown. It is obvious from these figures that $\langle P_L \rangle$ ($\langle P_N \rangle$) is weakly (strongly) sensitive to ξ while $\langle P_T \rangle$ is totally insensitive to ξ . We also note that $\langle P_N \rangle$ is zero in the SM and it is at the order of 1% in model IV for $\tan\beta = 30$. Thus, measurement of this component in future experiments may provide information about the model IV parameters.

Figs. (14)-(26) are devoted to the $B \rightarrow K^* \tau^+ \tau^-$ decay. In Fig.(14), dependence of the dBR/ds on s is given. We see that dBR/ds of this process is not as sensitive to the effects of NHB exchanges as $B \rightarrow K \tau^+ \tau^-$ decay and these effects begin to be significant when $\tan\beta > 40$.

In Fig. (15) and Fig. (16), $A_{FB}(s)$ and $\langle A_{FB} \rangle$ of $B \rightarrow K^* \ell^+ \ell^-$ as a function of s and CP violating phase ξ are presented. As in $B \rightarrow K \tau^+ \tau^-$ decay, A_{FB} here is also quite sensitive to $\tan\beta$, and its magnitude gets smaller than the SM prediction with the increasing values of $\tan\beta$. As seen from Fig. (16), $\langle A_{FB} \rangle$ in $B \rightarrow K^* \ell^+ \ell^-$ is of the order of 10% and strongly dependent on ξ , especially when $\tan\beta = 50$.

Fig. (17) and Fig. (18) show the dependence of $A_{CP}(s)$ on s and $\langle A_{CP} \rangle$ on ξ for $B \rightarrow K^* \tau^+ \tau^-$ decay. We see that $A_{CP}(s)$ is quite sensitive to $\tan\beta$ and ξ and it does not change sign in the allowed values of s . It follows from Fig. (18) that $\langle A_{CP} \rangle$ is of the order of 0.1% and hard to observe.

$A_{CP}(A_{FB})(s)$ and $\langle A_{CP}(A_{FB}) \rangle$ of $B \rightarrow K^* \tau^+ \tau^-$ as a function of s and CP violating

phase ξ are presented in Fig. (19) and Fig. (20), respectively. We see that $A_{CP}(A_{FB})$ comes mainly from exchanging NHBs and its magnitude can reach 0.3 exhibiting a strong dependence on the CP-violating phase ξ .

In Figs. (21)-(23), we present the s dependence of the longitudinal P_L , transverse P_T and normal P_N polarizations of the final lepton for $B \rightarrow K^* \tau^+ \tau^-$ decay. We see that NHB exchanges modify the spectrums of P_T and P_N greatly while its effect is relatively weak for P_L . We also observe that except the ψ' region, P_L is negative for all values of s , but P_T and P_N change sign with the different choices of the values of $\tan \beta$. In Figs. (24)-(26), dependence of the averaged values of the longitudinal $\langle P_L \rangle$, transverse $\langle P_T \rangle$ and normal $\langle P_N \rangle$ polarizations of the final lepton for $B \rightarrow K^* \ell^+ \ell^-$ decay on ξ are depicted. It is obvious from these figures that $\langle P_L \rangle$, $\langle P_T \rangle$ and $\langle P_N \rangle$ in model IV are larger as absolute values than the corresponding SM predictions. Sensitivity of these observables to the parameter ξ is significant when $\tan \beta$ is not smaller than 30.

We now summarize our results:

- We observe an enhancement in the differential branching ratio for both $B \rightarrow K \tau^+ \tau^-$ and $B \rightarrow K^* \tau^+ \tau^-$ processes in model IV compared to the SM when the NHB effects are taken into account. The NHB effects are more manifest in $B \rightarrow K \tau^+ \tau^-$ decay with respect to $B \rightarrow K^* \tau^+ \tau^-$ decay.
- A_{FB} comes only from NHB contributions in $B \rightarrow K \tau^+ \tau^-$, and its average is between $(-0.04, -0.01)$, which is non zero but hard to observe. However for $B \rightarrow K^* \tau^+ \tau^-$ decay, it is of the order of 10%, which should be within the luminosity reach of coming B factories.
- $\langle A_{CP} \rangle$ is between $(-0.8, 0.8) \times 10^{-2}$ and $(-0.3, 0.3) \times 10^{-2}$ in $B \rightarrow K \tau^+ \tau^-$ and $B \rightarrow K^* \tau^+ \tau^-$ decays, respectively. Since A_{CP} for these decays is practically zero in the SM, a nonzero value measured in future experiments for A_{CP} will be a definite indication of the existence of new physics.
- $A_{CP}(A_{FB})$ is at the order of 1% for $B \rightarrow K \tau^+ \tau^-$ decay and it is very sensitive to the CP violating phase ξ , but not to $\tan \beta$. As for $B \rightarrow K^* \tau^+ \tau^-$ decay, it comes mainly from exchanging NHBs, and can be as large as 30% for some values of ξ .
- Model IV contributions modify the spectrums of P_L , P_T and P_N greatly compared to the SM case for both decays. These quantities are sensitive to the NHB effect and also the CP violating phase ξ , except the P_T component for $B \rightarrow K \tau^+ \tau^-$ decay.

Therefore, the experimental investigation of A_{FB} , A_{CP} , $A_{CP}(A_{FB})$ and the polarization components in $B \rightarrow K \ell^+ \ell^-$ and $B \rightarrow K^* \ell^+ \ell^-$ decays may be quite suitable for testing the new physics effects beyond the SM.

Acknowledgement

We would like to thank Shou Hua Zhu for his comments about the previous version of this work.

References

- [1] B.Grinstein, M.J.Savage and M.B.Wise, *Nucl. Phys.***B 319**(1989) 271.
- [2] N. G. Deshpande, X. -G. He and J. Trampetic, *Phys. Lett. B* **367** (1996) 362 .
- [3] Y.B. Dai, C.S. Huang and H.W. Huang, *Phys. Lett.***B 390**(1997) 257.
- [4] C.S. Huang and Q.S. Yan, *Phys. Lett.***B 442**(1998) 209; C.S. Huang, W. Liao and Q.S. Yan, *Phys. Rev.***D 59**(1999) 011701;
- [5] S. Fukae, C.S. Kim and T. Yoshikawa, hep-ph/9908229.
- [6] S. Fukae, C.S. Kim, T. Morozumi and T. Yoshikawa, *Phys. Rev.***D 59**(1999) 074013.
- [7] Y.G. Kim, P.Ko, and J.S. Lee, *Nucl. Phys.***B 544** (1999) 64.
- [8] T. Goto *et.al.*, *Phys. Rev.***D 55** (1997) 4273; T. Goto, Y. Okada and Y. Shimizu, *Phys. Rev.***D 58** (1998)094006.
- [9] E. Lunghi *et.al.*, *Nucl. Phys.***B 568** (2000) 120 , and references therein.
- [10] J. L. Hewett, *Phys. Rev.***D 53** (1996)4964.
- [11] Y. Grossman, Z. Ligeti and E. Nardi, *Phys. Rev.***D 55** (1997)2768.
- [12] K. Krüger and L.M. Sehgal, *Phys. Lett.***B 380**(1996)199.
- [13] I.I. Bigi, M. Shifman, N.G. Vraltsev and A.I. Vainstein, *Phys. Rev. Lett.* **71** (1993) 496; B. Blok, L. Kozrakh, M. Shifman and A.I. Vainstein, *Phys. Rev.***D 49** (1994) 3356; A.V. Manohar and M.B. Wise, *Phys. Rev.***D 49** (1994)1310; S. Balk, T.G. Körner, D. Pirjol and K. Schilcher, *Z. Phys. C* **64** (1994) 37; A.F. Falk, Z. Ligeti, M. Neubert and Y. Nir, *Phys. Lett.***B 326**(1994)145.
- [14] R. Casalbuoni, A. Deandra, N. Di Bartolemo, R. Gatto and G. Nardulli, *Phys. Lett. B* **312** (1993) 315.
- [15] P. Colangelo, F. De Fazio, P. Santorelli and E. Scrimieri, *Phys. Rev. D* **53** (1996) 3672; Erratum, *ibid.* **D57** (1998) 3186.
- [16] W. Jaus and D. Wyler, *Phys. Rev. D* **41** (1990) 3405.
- [17] W. Roberts, *Phys. Rev. D* **54** (1996) 863.
- [18] T. M. Aliev, A. Özpineci and M. Savcı, *Phys. Rev. D* **56** (1997) 4260.
- [19] P. Ball and V. M. Braun, *Phys. Rev. D* **58** (1998) 094016.
- [20] CDF Collaboration, T. Affolder *et al*, *Phys. Rev. Lett.* **83** (1999) 3378 .
- [21] K. Abe,*et al* Belle Collaboration, *Phys. Rev. Lett.* **88**(2002) 021801 .
- [22] N.G. Deshpande and J. Trampetić, *Phys. Rev. Lett.* **60** (1988)2583.
- [23] P. J. O'Donnell and H. K. Tung, *Phys. Rev. D* **43** (1991) 2067 .
- [24] D.S. Du and C. Liu, *Phys. Lett. B* **317** (1993) 179.
- [25] G. Burdman, *Phys. Rev. D* **52** (1995) 6400; W. Roberts, *Phys. Rev. D* **54** (1996) 863.
- [26] D.S. Liu ,*Phys. Rev. D* **52** (1995) 5056;
- [27] C. Greub, A.Ioannissian, and D.Wyler, *Phys. Lett.B* 3461995149.
- [28] C.Q. Geng and C.P Kao, *Phys. Rev. D* **54**(1996) 5636.
- [29] D. Melikhov, N. Nikitin, and S. Simula, *Phys. Lett. B* **442** (1998) 381.

- [30] T. M. Aliev, M. Savci, A. Özpineci, and H. Koru; *J. Phys.* **G 24** (1998) 49.
- [31] T. M. Aliev and E. O. Iltan, *Phys. Lett.* **B 451** (1998) 175.
- [32] A. Ali, P. Ball, L.T. Handoko, G. Hiller, *Phys. Rev.* **D 61** (2000) 074024.
- [33] F. Krüger and J. C. Romão, *Phys. Rev.* **D 62** (2000) 034020.
- [34] T.M. Aliev, C.S. Kim and Y.G. Kim, *Phys. Rev.* **D 62** (2000) 014026.
- [35] T.M. Aliev and M. Savci, *Phys. Lett.* **B 481** (2000) 275.
- [36] T. M. Aliev, A. Özpineci, M. Savci, *Phys.Lett. B* **511** (2001) 49.
- [37] E. O. Iltan, hep-ph/0102061 (2001)
- [38] D. Guetta and E. Nardi, *Phys. Rev.* **D 58** (1998) 012001.
- [39] C.-S. Huang and S. H. Zhu *Phys. Rev.* **D 61** (1999) 015011 ; erratum *ibid.* **D 61**(2000) 119903 .
- [40] D. Buskulic, *et all.*, ALEPH Collaboration, *Phys. Lett.* **B 343** (1995) 444; J. Kalinowski, *Phys. Lett.* **B 245** (1990) 201; A. K. Grant, *Phys. Rev.* **D 51** (1995) 207.
- [41] T. M. Aliev, M. K. Cakmak and M. Savci, *Phys. Rev.* **D 64** (2001) 055007.
- [42] T. M. Aliev, M. K. Cakmak and M. Savci, *Nucl.Phys. B* **607** (2001) 305.
- [43] Q.-S. Yan, C.-S. Huang, W. Liao and S. H. Zhu *Phys. Rev.* **D 62** (2000) 094023.
- [44] Y. B. Dai, C. S. Huang and H. W. Huang, *Phys. Lett.* **B 390** (1997) 257; erratum **B 513** (2001) 429 ;C. S. Huang, L. Wei and Q. S. Yan , *Phys. Rev.* **D 59** (1999) 011701.
- [45] C. S. Huang, L. Wei, Q. S. Yan and S. H. Zhu, *Phys. Rev.* **D 63** (2001) 114021.
- [46] H. E. Logan and U. Nierste, *Nucl. Phys.* **B 586** (2000) 39.
- [47] C. Bobeth, T. Ewerth, F. Krüger and J. Urban, *Phys. Rev.* **D 64** (2001) 074014.
- [48] Z. Xiong and J. M. Yang. *hep-ph/0105260*
- [49] C. S. Huang, L. Wei, Q. S. Yan and S. H. Zhu, *Phys. Rev.* **D 64** (2001) 059902.
- [50] B. Grinstein, R. Springer, and M. B. Wise, *Nucl. Phys.* **B339** (1990) 269; R. Grigjanis, P.J. O'Donnell, M. Sutherland and H. Navelet, *Phys. Lett.* **B 213** (1988) 355; *Phys. Lett.* **B 286** (1992) , 413; G. Cella, G. Curci, G. Ricciardi and A. Viceré, *Phys. Lett.* **B 325** (1994) 227; *Nucl. Phys.* **B 431** (1994) 417.
- [51] A. J. Buras and M. Münz, *Phys. Rev.* **D 52** (1995) 186; M. Misiak, *Nucl. Phys.*, **B 393**(1993) 23; erratum *ibid.* **B 439** (1995) 461.
- [52] A. Ali, T. Mannel and T. Morozumi, *Phys. Lett.* **B 273** (1991) 505;
- [53] A. Heister, *et al*, ALEPH Collaboration, CERN-EP/2001-095; L3 Collaboration, *Phys. Lett.* **B 503** (2001) 21.

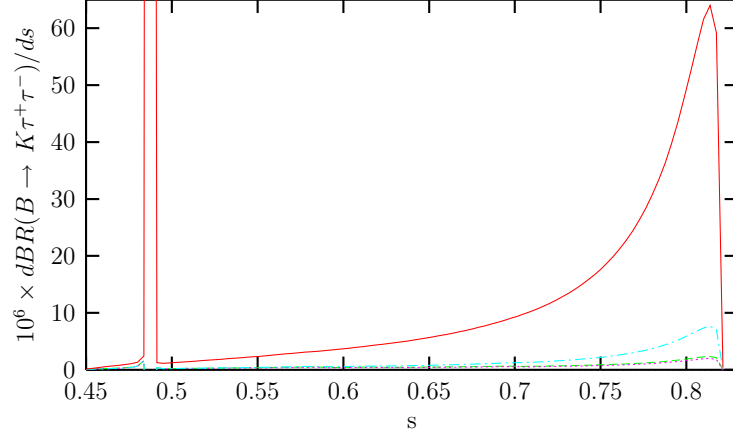


Figure 1: The dependence of the dBR/ds on s for $B \rightarrow K\tau^+\tau^-$ decay. Here dot lines, dashed-dot lines and solid lines represent the model IV contributions with $\tan\beta = 10, 30, 50$, respectively and the dashed lines are for the SM predictions.

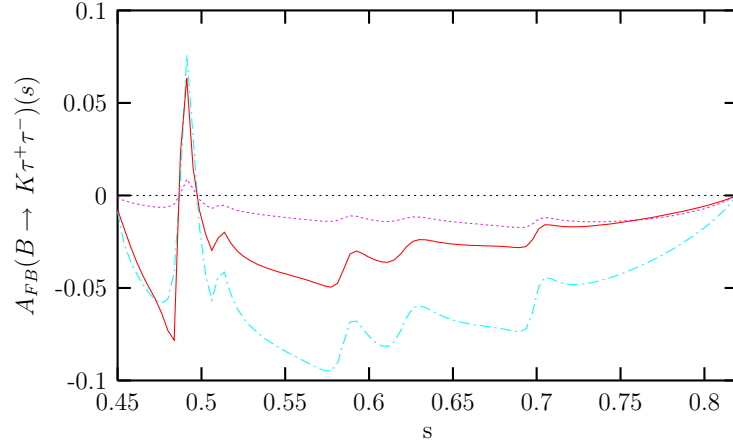


Figure 2: The dependence of $A_{FB}(s)(B \rightarrow K\tau^+\tau^-)$ on s . Here dot lines, dashed-dot lines and solid lines represent the model IV contributions with $\tan\beta = 10, 30, 50$, respectively and the dashed lines are for the SM predictions.

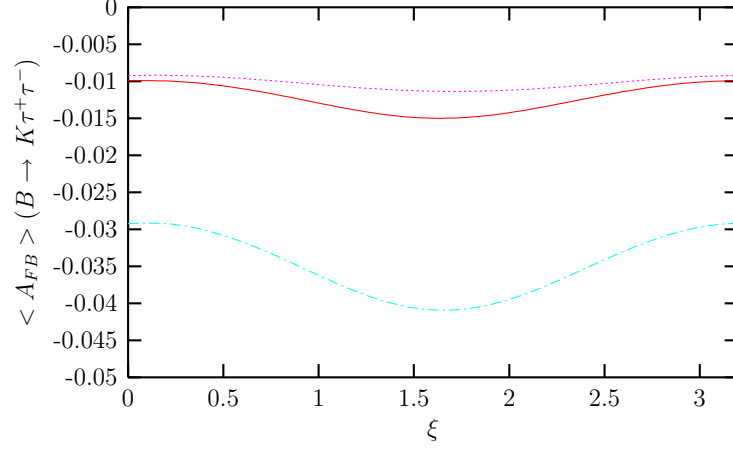


Figure 3: The dependence of $\langle A_{FB} \rangle (B \rightarrow K\tau^+\tau^-)$ on ξ . Here dot lines, dashed-dot lines and solid lines represent the model IV contributions with $\tan\beta = 10, 30, 50$, respectively and the dashed lines are for the SM predictions.

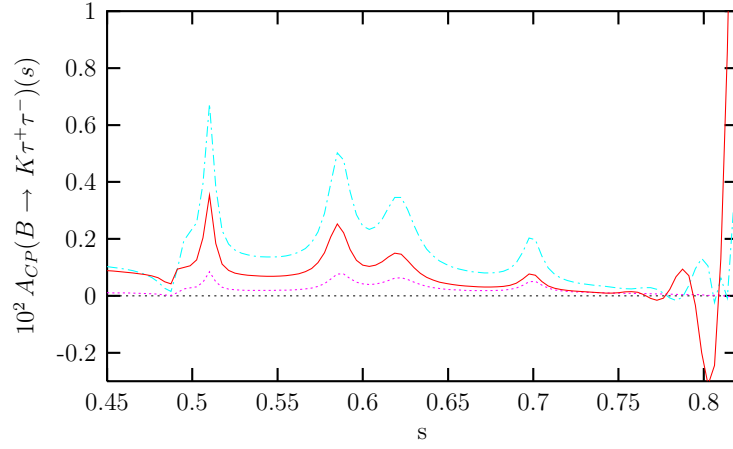


Figure 4: The same as Fig.(2), but for $A_{CP}(s)(B \rightarrow K\tau^+\tau^-)$.

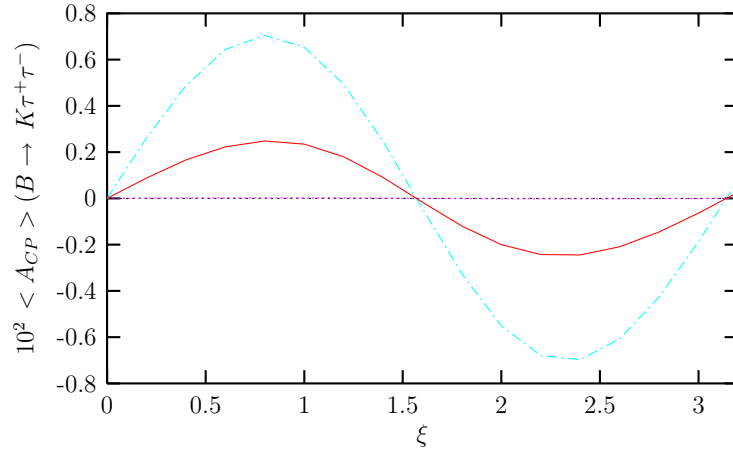


Figure 5: The same as Fig.(3), but for $\langle A_{CP} \rangle (B \rightarrow K\tau^+\tau^-)$.

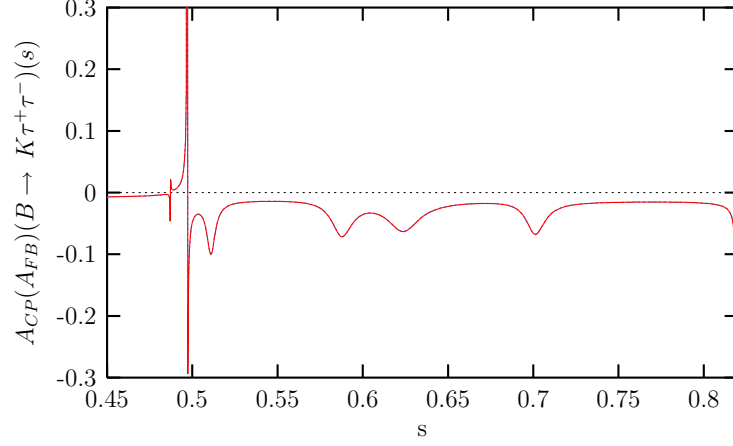


Figure 6: The same as Fig.(2), but for $A_{CP}(A_{FB})(s)(B \rightarrow K\tau^+\tau^-)$.

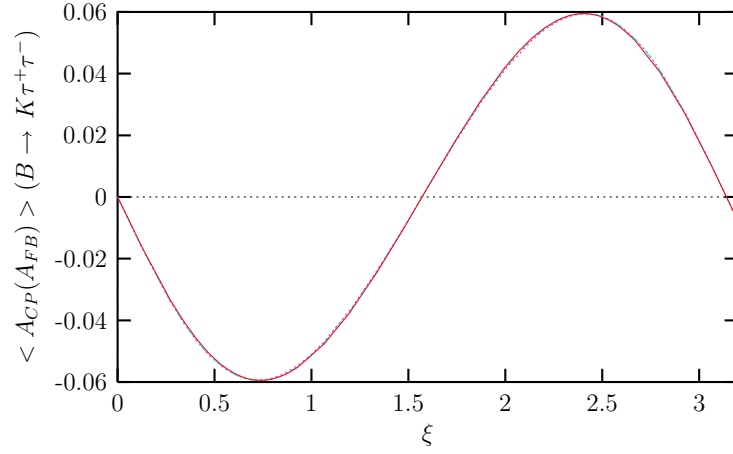


Figure 7: The same as Fig.(3), but for $\langle A_{CP}(A_{FB}) \rangle (B \rightarrow K\tau^+\tau^-)$.

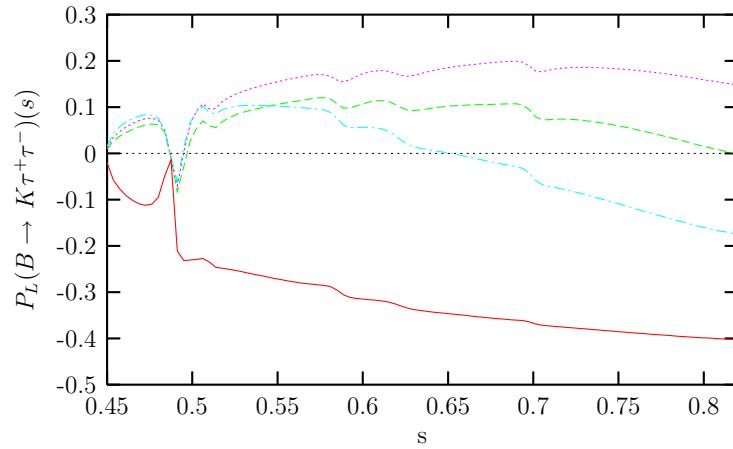


Figure 8: The dependence of $P_L(s)(B \rightarrow K\tau^+\tau^-)$ on s . Here dot lines, dashed-dot lines and solid lines represent the model IV contributions with $\tan \beta = 10, 30, 50$, respectively and the dashed lines are for the SM predictions.

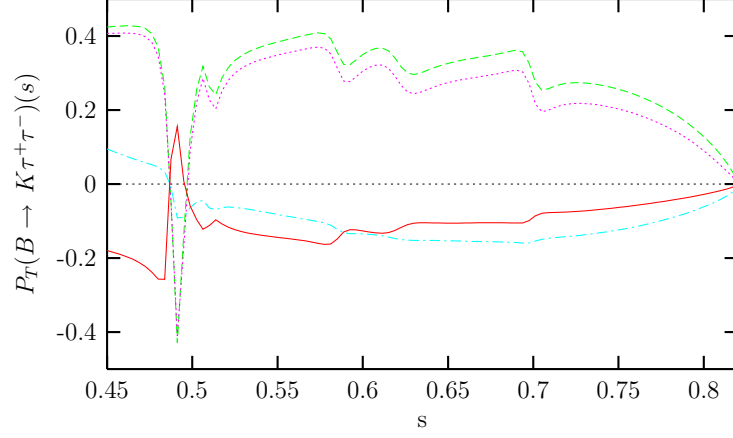


Figure 9: The same as Fig.(8), but for $P_T(s)(B \rightarrow K\tau^+\tau^-)$.

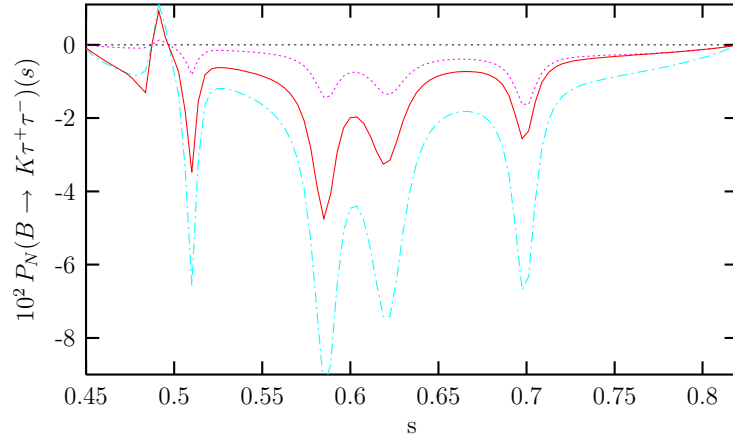


Figure 10: The same as Fig.(8), but for $P_N(s)(B \rightarrow K\tau^+\tau^-)$.

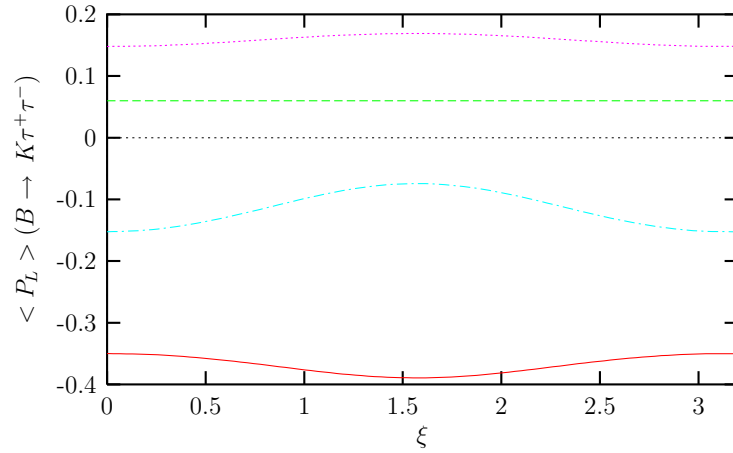


Figure 11: The dependence of $\langle P_L \rangle (B \rightarrow K\tau^+\tau^-)$ on ξ . Here dot lines, dashed-dot lines and solid lines represent the model IV contributions with $\tan \beta = 10, 30, 50$, respectively and the dashed lines are for the SM predictions.

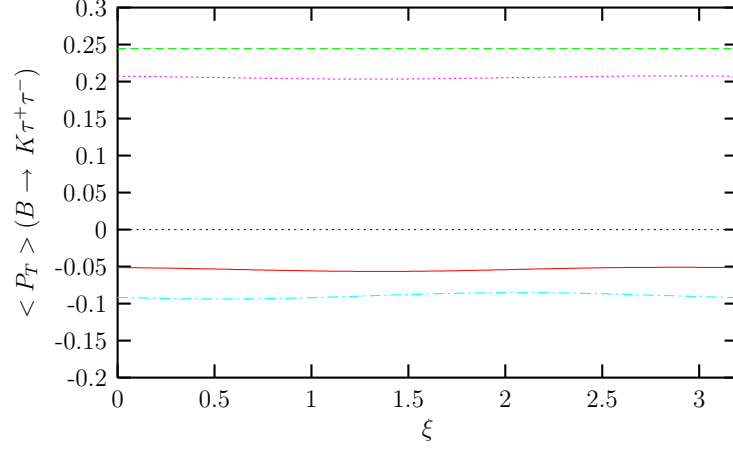


Figure 12: The same as Fig.(11), but for $\langle P_T \rangle (B \rightarrow K\tau^+\tau^-)$.

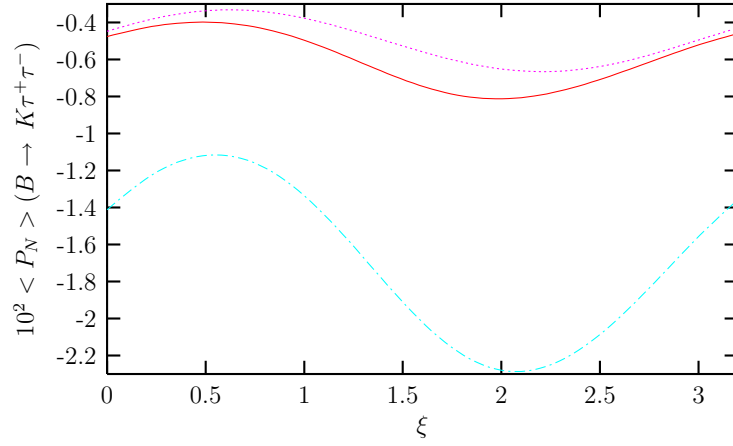


Figure 13: The same as Fig.(11), but for $\langle P_N \rangle (B \rightarrow K\tau^+\tau^-)$.

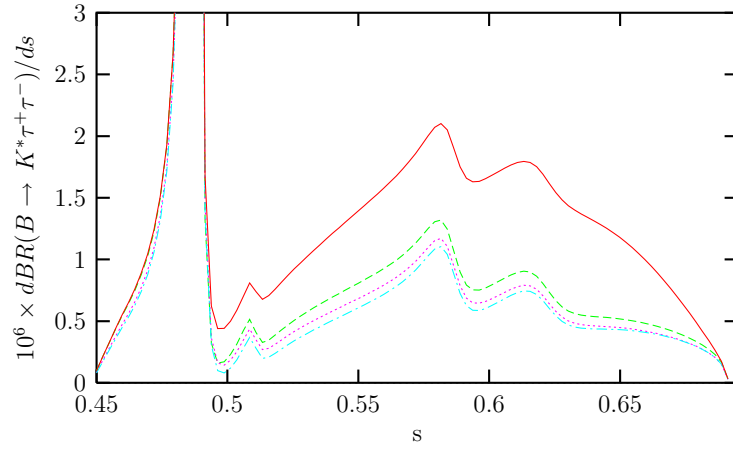


Figure 14: The dependence of the dBR/ds on s for $B \rightarrow K^*\tau^+\tau^-$ decay. Here dot lines, dashed-dot lines and solid lines represent the model IV contributions with $\tan \beta = 10, 30, 50$, respectively and the dashed lines are for the SM predictions.

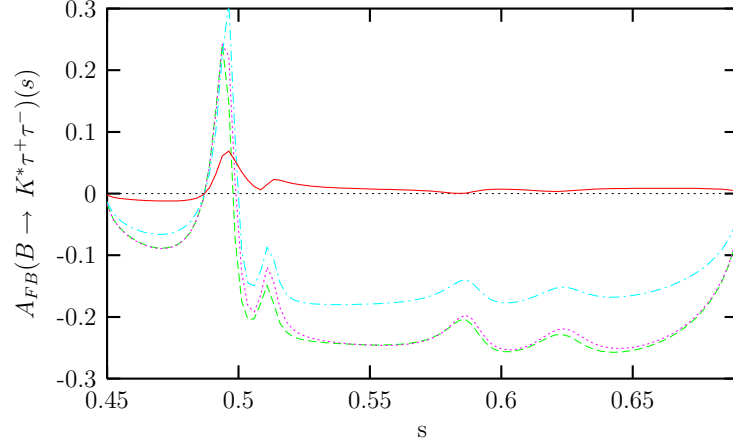


Figure 15: The dependence of $A_{FB}(s)(B \rightarrow K^*\tau^+\tau^-)$ on s . Here dot lines, dashed-dot lines and solid lines represent the model IV contributions with $\tan\beta = 10, 30, 50$, respectively and the dashed lines are for the SM predictions.

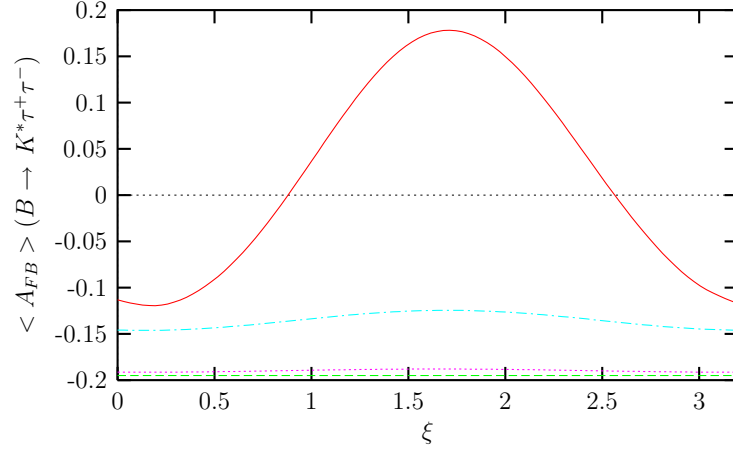


Figure 16: The dependence of $\langle A_{FB} \rangle (B \rightarrow K^*\tau^+\tau^-)$ on ξ . Here dot lines, dashed-dot lines and solid lines represent the model IV contributions with $\tan\beta = 10, 30, 50$, respectively and the dashed lines are for the SM predictions.

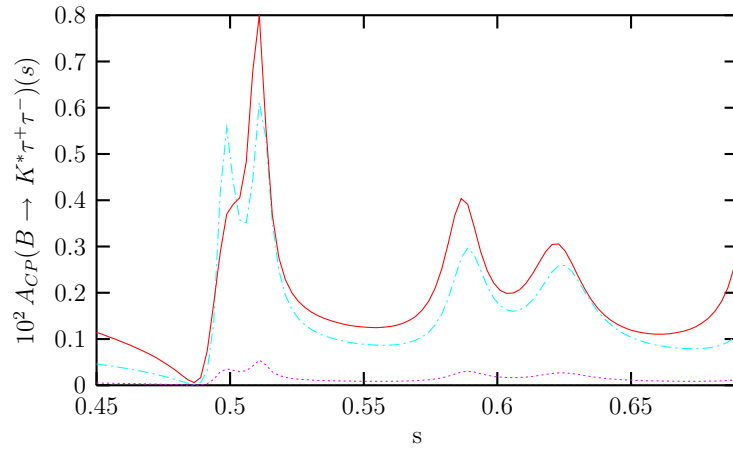


Figure 17: The same as Fig.(15), but for $A_{CP}(s)(B \rightarrow K^*\tau^+\tau^-)$.

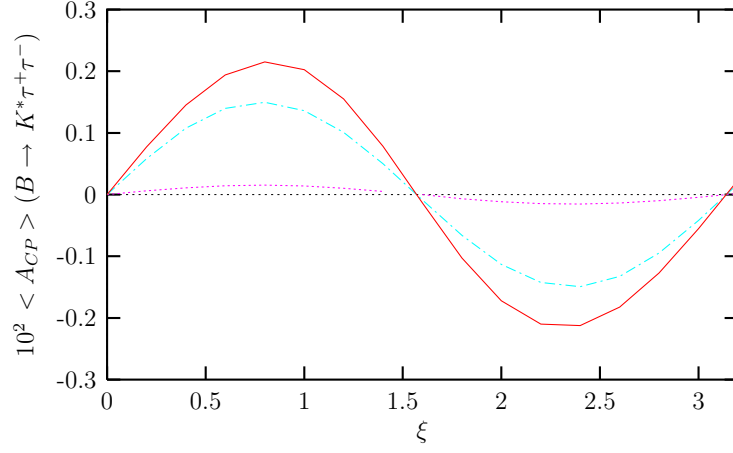


Figure 18: The same as Fig.(16), but for $\langle A_{CP} \rangle (B \rightarrow K^* \tau^+ \tau^-)$.

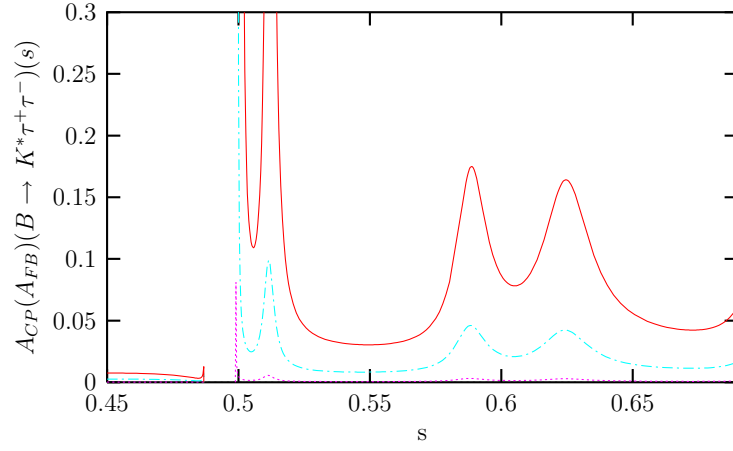


Figure 19: The same as Fig.(15), but for $A_{CP}(A_{FB})(s)(B \rightarrow K^* \tau^+ \tau^-)$.

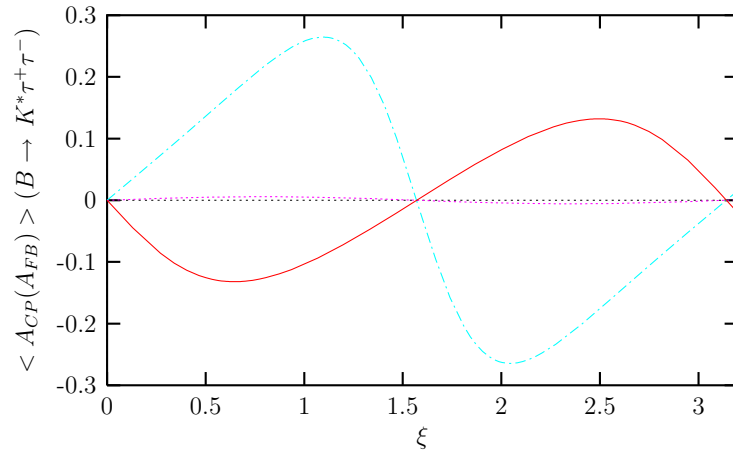


Figure 20: The same as Fig.(16), but for $\langle A_{CP}(A_{FB}) \rangle (B \rightarrow K^* \tau^+ \tau^-)$.

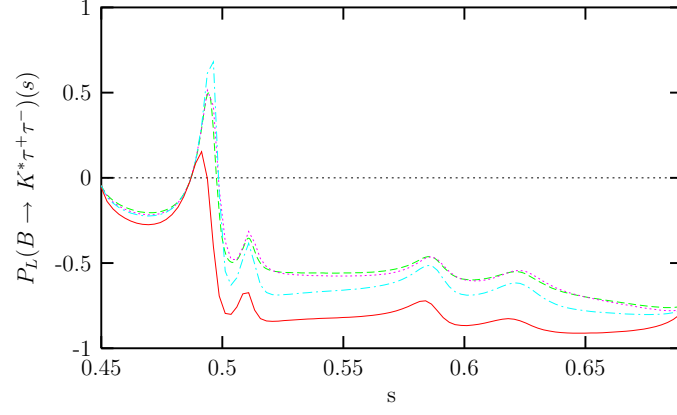


Figure 21: The dependence of $P_L(s)(B \rightarrow K^* \tau^+ \tau^-)$ on s . Here dot lines, dashed-dot lines and solid lines represent the model IV contributions with $\tan \beta = 10, 30, 50$, respectively and the dashed lines are for the SM predictions.

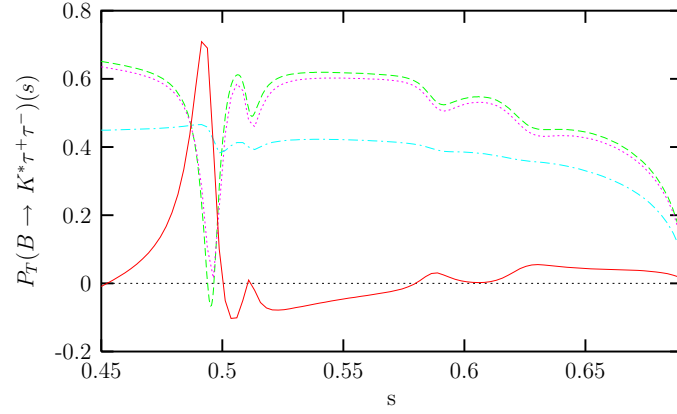


Figure 22: The same as Fig.(21), but for $P_T(s)(B \rightarrow K^* \tau^+ \tau^-)$.

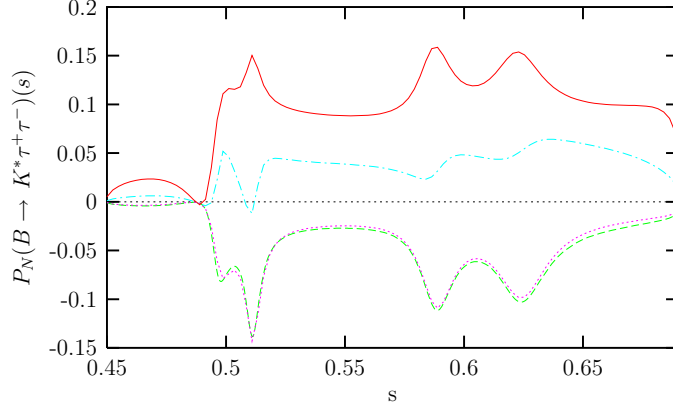


Figure 23: The same as Fig.(21), but for $P_N(s)(B \rightarrow K^*\tau^+\tau^-)$.

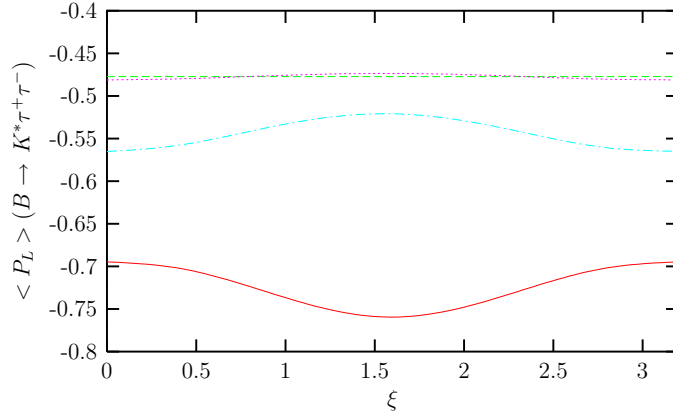


Figure 24: The dependence of $\langle P_L \rangle (B \rightarrow K^*\tau^+\tau^-)$ on ξ . Here dot lines, dashed-dot lines and solid lines represent the model IV contributions with $\tan \beta = 10, 30, 50$, respectively and the dashed lines are for the SM predictions.

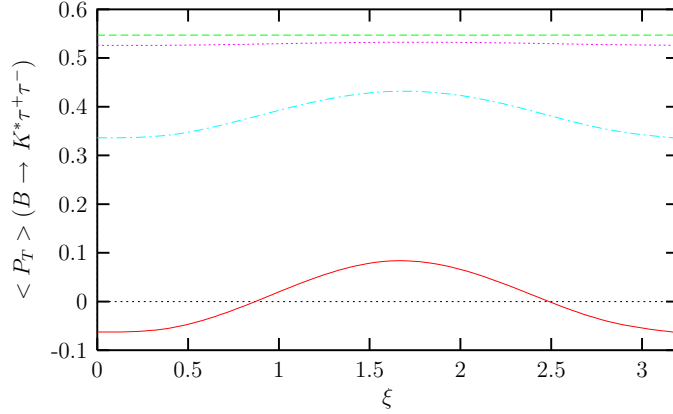


Figure 25: The same as Fig.(24), but for $\langle P_T \rangle (B \rightarrow K^*\tau^+\tau^-)$.

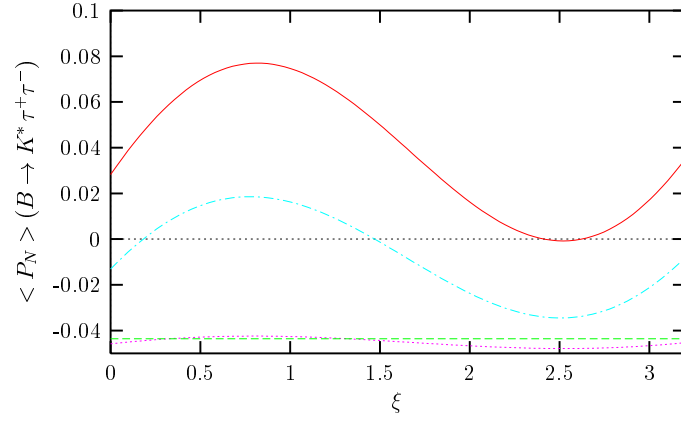


Figure 26: The same as Fig.(24), but for $\langle P_N \rangle (B \rightarrow K^* \tau^+ \tau^-)$.